JPE 16-1-17

http://dx.doi.org/10.6113/JPE.2016.16.1.153
ISSN(Print): 1598-2092 / ISSN(Online): 2093-4718

Simple Technique Reducing Leakage Current for H-Bridge Converter in Transformerless Photovoltaic Generation

Radoslaw Kot†, Sebastian Stynski*, Krzysztof Stepien**, Jaroslaw Zaleski**, and Mariusz Malinowski*

†,*Institute of Control and Industrial Electronics, Warsaw University of Technology, Warsaw, Poland
**ZE TWERD Power Electronics Company, Torun, Poland

Abstract

Given their structural arrangement, photovoltaic (PV) modules exhibit parasitic capacitance, which creates a path for high-frequency current during zero-state switching of the converter in transformerless systems. This current has to be limited to ensure safety and electromagnetic compatibility. Many solutions that can minimize or completely avoid this phenomenon, are available. However, most of these solutions are patented because they rely on specific and often complex converter topologies. This study aims to solve this problem by introducing a solution based on a classic converter topology with an appropriate modulation technique and passive filtering. A 5.5 kW single-phase residential PV system that consists of DC-DC boost stage and DC-AC H-bridge converter is considered. Control schemes for both converter stages are presented. An overview of existing modulation techniques for H-bridge converter is provided, and a modification of hybrid modulation is proposed. A system prototype is built for the experimental verification. As shown in the study, with simple filtering and proper selection of switching states, achieving low leakage current level is possible while maintaining high converter efficiency and required energy quality.

Key words: Leakage currents, Pulse width modulation (PWM), Renewable energy

I. INTRODUCTION

Photovoltaic (PV) modules are the structural basic unit for PV systems, comprised of PV cells. Modules can be connected in series and in parallel to form large structures called PV arrays. This feature allows the development of scalable systems, from small-scale domestic applications ranging from a few kilowatts to large-scale power plants with capacities in orders of tens to hundreds of megawatts. The first category is especially popular because of the declining costs of installation and system components. Government support in the form of subsidies and green tariffs has driven development in many countries. This process initiated an ongoing growth in the field of PV power converters. Many new solutions emerged, including converter topologies, monitoring systems, and control algorithms. Power converters for PV applications have become a dedicated group with many specific functions integrated in their control structures. Well-established and inherently embedded features, such as maximum power point tracking (MPPT), anti-islanding, ride-through grid disturbances, current harmonics compensation, and advanced synchronization, were either developed or highly improved. Efficient energy processing is the most important design criteria in every energy conversion stage because of the relatively low efficiency of modules (between 14% and 18% for commercially available polycrystalline modules). Therefore, minimizing the number of these stages has become reasonable by considering highly efficient systems has become reasonable. Initially, this process was performed mostly by eliminating the low-frequency transformer, which, despite providing galvanic isolation and voltage level adjustment, is characterized by high cost and relatively low

Manuscript received May 4, 2015; accepted Jun. 30, 2015
Recommended for publication by Associate Editor Liqiang Yuan.
†Corresponding Author: radoslaw.kot@ee.pw.edu.pl
Tel: +48-22-234-5485, Fax: +48-22-234-6023, Warsaw Univ. of Tech.
*Institute of Control and Industrial Electronics, Warsaw University of Technology, Poland
**ZE TWERD Power Electronics Company, Poland

energy density. The introduction of high-frequency transformers with a much higher energy density was inevitably associated with the addition of a DC-DC conversion stage with numerous passive and active components. Therefore, transformerless systems, with their primary design guideline, became popular. Transformerless systems demonstrate reduced cost and size compared with conventional systems. However, major issues exist with regard to the operation of such systems. First, lack of galvanic isolation of these systems imposes some concerns about safety issues. Unfortunately, PV modules exhibit non-negligible parasitic capacitance, which is formed between the module substrate and its grounded frame. For transformerless systems, this phenomenon creates a capacitive link between the grid and the PV modules, which can provide a path for high-frequency current component formed by the switching action of the converter. This current closes its path through the ground, thereby compromising human safety and causing additional electromagnetic interference problems [1], [2]. Second, the lack of galvanic isolation allows a DC current component to be injected to the grid, which is limited or restricted in many grid codes [3].

In the following sections, problems related to the operation of transformerless converters are explained. Subsequently, a novel technique for minimizing the leakage current phenomena is presented, and experimental verification is provided.

II. Common-Mode Voltage and Current

Common-mode voltage v_{CM} is defined as the mean value of converter terminal voltages v_{A0} and v_{B0}, i.e., voltages of each leg referenced to the negative DC terminal (see Fig. 1), which for single-phase converters is equal to:

$$v_{CM} = \frac{v_{A0} + v_{B0}}{2}. \quad (1)$$

To obtain high efficiency, a modulation scheme that allows unipolar switching (i.e., adopting zero-voltage states) has to be utilized. However, if zero-voltage states are applied in the pulse-width modulation (PWM) scheme, converter terminals become effectively shortened for a fraction of a switching period, thus introducing unwanted v_{CM} variations. A variation is not an issue, unless a galvanic connection between PV array and the grid exists, which is the case for transformerless systems.

PV modules generally consist of the encapsulated semiconductor structure and aluminum grounded frame. Such arrangement naturally creates capacitance C_{PV} between these elements and ground, which varies significantly with environmental conditions, particularly humidity of the modules. The values are usually expressed relative to array power and can range from several nF/kW up to few μF/kW [4], [5]. The current that flows in the presence of this

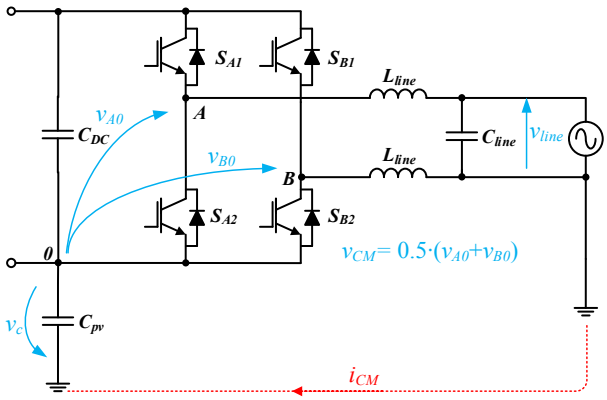

Fig. 1. Grid-connected H-bridge converter.

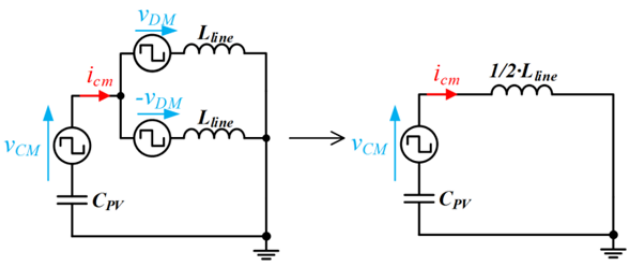

Fig. 2. Simplified converter model for leakage current analysis.

capacitance is called common-mode current i_{CM} or leakage current. Its path goes through the PV module, ground connection, and converter output filter (Fig. 1). Common-mode current i_{CM} introduces electromagnetic interference, grid current, distortion, and potential electric hazards. Leakage current is also caused by grid voltage variations; however, because of its low frequency (relative to the switching frequency), its value becomes insignificant. Leakage current phenomena can be modeled as follows: Given that differential voltage of the converter is equal, then

$$v_{DM} = v_{A0} - v_{B0}, \quad (2)$$

and by neglecting the grid voltage contribution to the leakage current, terminal voltages v_{A0} and v_{B0} can be expressed in terms of v_{CM} and v_{DM} as

$$v_{A0} = \frac{v_{DM}}{2} + v_{CM} \quad (3)$$

and

$$v_{B0} = -\frac{v_{DM}}{2} + v_{CM}. \quad (4)$$

This corresponds to the converter representation shown in Fig. 2(a). Assuming equal inductor values in both converter legs (balanced system), the differential voltage has no effect on the leakage current. Therefore, the converter can be modeled as shown in Fig. 2(b). Reducing the value of the leakage current to an acceptable limit requires minimizing the common-mode voltage variation during the switching period of the converter. The v_{CM} waveform depends on the modulation schemes and the value of DC-link voltage V_{DC}.

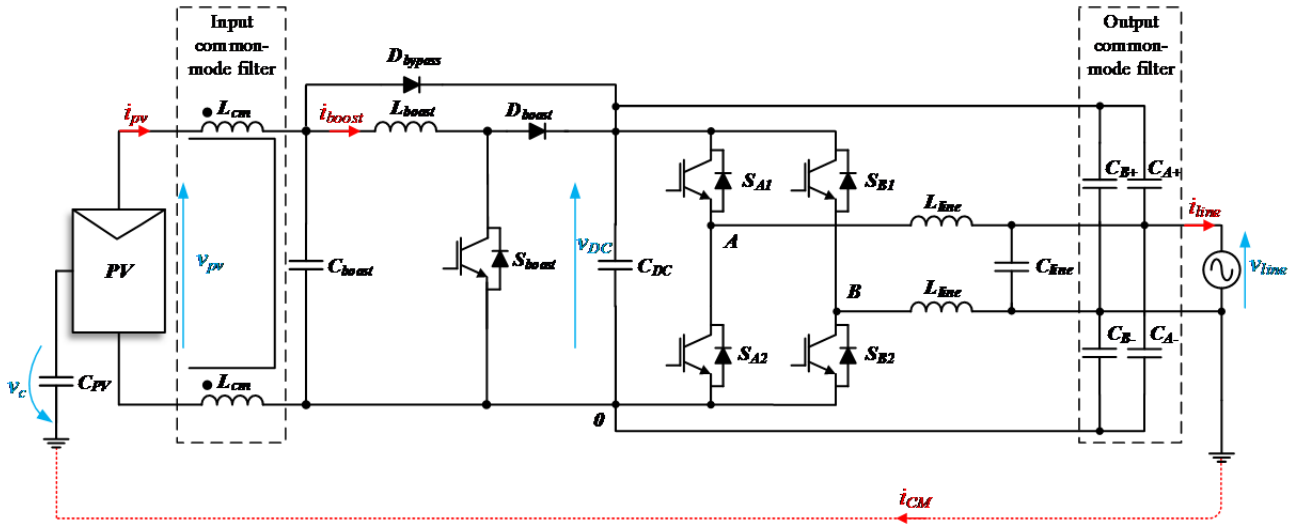

Fig. 3. Proposed system with H-bridge and boost converters, common-mode filter, and modeled parasitic capacitance C_{PV}.

Several methods can be employed to minimize this problem. The simplest one is to adopt a modulation technique that does not allow for any zero-voltage states. Unfortunately, using this method decreases efficiency and increases the size of a grid-side filter. The second method involves disconnecting the converter from the PV array (either on the DC or AC side) during zero-voltage states [6], [7]. In this manner, the common-mode voltage still varies, but a path for leakage current flow does not exist. This solution implies utilizing additional switches, but it has been widely adopted for transformerless PV topologies by many power electronics companies [3], [7]. The three most commonly recognized topologies are H5 by SMA, HERIC by Sunways, and FB-DCBP by Ingeteam. These solutions are difficult to implement in new products because of existing patents. Moreover, as shown in [8], some topologies with additional bypass switches may also cause v_{CM} variations during low-voltage ride-through (LVRT) operation, which has recently become of interest for PV systems.

Another solution is to change the topology of the DC-AC converter from classical H-bridge to half-bridge diode clamped topology because of their fixed connection between PV array and ground. The half-bridge diode clamped topology does not require any additional elements but needs at least two times higher DC-link voltage to operate normally.

III. Proposed System

Another approach has been taken to avoid restrictions related to the abovementioned topologies. It focuses on modulation techniques that reduce CM voltage variations for the converter rather than techniques that modify the existing topology itself. In addition, small common-mode filters are necessary to maintain a low RMS value of the leakage current below 300 mA (limit set according to VDE0126-1-1 standard). In addition to minimizing the leakage current, the PV converter has to fulfill many important requirements to be suitable for high-performance industrial applications. The most desirable features can be depicted as [9].

- THD of the line current below 5% (IEEE 1547, IEC 61727);
- high efficiency (over 97%);
- control simplicity.

A. Power Circuit

The power stage of the proposed 5.5-kW system is shown in Fig. 3. The system consists of DC-DC (boost topology) and DC-AC (H-bridge) converters, which are considered simple, robust, and relatively cheap. A diode bypassing DC-DC stage is adopted to conduct a current in case the PV voltage exceeds the DC-link voltage. Moreover, the power circuit of the converter was extended with two additional common-mode filters [10], which are necessary to limit the maximum value and slew rate of a leakage current. Common-mode inductive filter L_{cm} is placed at the input stage of the boost converter. It limits the slew rate of a leakage current, and it turn reduces its RMS value. The second filter is composed of two capacitor banks at the output stage of the H-bridge. Each bank is connected between two legs and corresponding DC terminals (positive or negative), which results in four additional capacitors: C_{A-}, C_{A+}, C_{B-}, and C_{B+}. The role of these capacitors is to close the path for a leakage current during zero-voltage states of the converter. However, these capacitors create a resonant tank, along with line inductors L_{line} and parasitic capacitance, which may lead to oscillations when fast v_{CM} change occurs, as will be shown in the next section.

B. Control Scheme of the DC-DC Converter

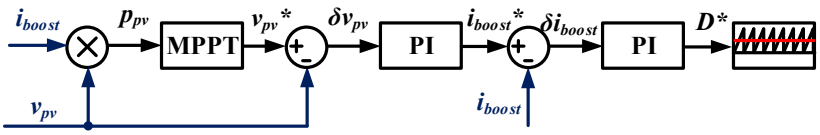

Fig. 4. Control scheme for the DC-DC boost converter.

The boost converter control is responsible for the extraction of the maximum available power of the PV plant (Fig. 4). The structure is obtained by the MPPT algorithm, which properly references the converter input voltage (PV voltage). For this study, perturb and observe (P&O) algorithm was used because of its simplicity [11]-[14]. The sign of a new step in voltage is selected based on the measurement of the change in power and previous perturbation in the PV voltage, with respect to which this change occurred. To achieve improved dynamics and a small steady-state error, variable step size referencing was implemented, which is simply based on the rate of the change of power with respect to applied voltage step [15]. When an actual operating point is far from the maximum power point (MPP), even a small perturbation in voltage results in a large change in power (large dp_{pv}/dv_{pv}).

Therefore, a large step size can be set to reduce the time taken to achieve MPP. However, when dp_{pv}/dv_{pv} is close to zero, no significant change in power will occur, and therefore, the step size is small, which reduces unnecessary oscillations and improves efficiency. Reference change in the PV voltage is realized by a PI controller, which provides a reference value for the inductor current. An inner-loop PI controller is responsible for maintaining the current by calculating a proper duty cycle for the converter switch.

C. Control Scheme of the DC-AC Converter

The control scheme for a DC-AC part, which is presented in Fig. 5, consists of two cascaded loops. The external voltage loop controls the power flow in the system by stabilizing the DC-link voltage. Reference DC-link voltage v_{DC}* is compared with the measured v_{DC} value. The v_{DC} voltage is distorted by a 100-Hz AC oscillation. This oscillation distorts the DC-link voltage δv_{DC} error signal because the v_{DC}* has a constant DC value. The v_{DC} PI regulator, which generates referenced grid current amplitude $i_{line,max}$, cannot eliminate the phase error. Thus, to prevent the transmission of 100 Hz distortion on $i_{line,max}$, a low-pass filter with 30 Hz cutoff frequency is applied to δv_{DC}. The internal current loop is responsible for the system power quality by controlling the grid current. The unity power factor operation can be achieved if reference grid current i_{line}* is in phase with line voltage v_{line}. For this purpose, synchronization with v_{line} is required. Among many methods [16], a phase-locked loop (PLL) based on second-order generalized integrator (SOGI) is utilized to generate v_{line} angle θ [17]. The SOGI is used to generate an in-quadrature signal of v_{line} required in a single-phase system to provide transformation into the synchronous reference frame. Reference grid current i_{line}* is compared with measured i_{line}, and error is delivered to the proportional multiresonant (PMR) controller [18, 19]. The PMR is composed of proportional gain and resonant integrator.

$$G(s) = K_p + \frac{K_i s}{s^2 + \omega^2} + \sum_h \frac{K_i s}{s^2 + (h\omega)^2} \tag{5}$$

where K_p and K_i are the gains for proportional and resonant part, respectively, ω is the v_{line} fundamental frequency, and h is the odd harmonic order of i_{line}. Such structure can track input phase-angle θ without a steady-state error with specified (e.g., 3rd, 5th, 7th, and 9th) higher current harmonics compensation by simply adding parallel connection—to the fundamental PR controller—resonant terms for specified $h\omega$ frequencies.

IV. Modulation Techniques for the H-Bridge Converter

A. State of the Art

The PWM technique used to generate output voltage v_{AB} of the converter highly influences its losses, quality of extracted energy, and, in a certain case, leakage current level. Three well-known modulation techniques for the H-bridge converter are described below to perform a comparative study. With no additional filtering, only bipolar PWM is suitable for the transformerless PV systems, but at the expense of efficiency. Next, an improvement in the hybrid modulation is presented, which ensures unipolar change in common-mode voltage v_{CM} (either from 0 to $V_{DC}/2$ or from $V_{DC}/2$ to V_{DC}). Thus, i_{cm} current reduction occurs, whereas high current spikes and oscillations generated in the presence of passive filters are avoided. Taking into consideration data sheet parameters for particular transistor and diode (see Section V for details) a per-unit switching loss calculation is also provided. Calculations were performed only for a relative loss evaluation, and detailed values are not shown. Power losses were calculated across only one switching period with a bipolar PWM set, which is the base for the comparison. Results are summarized in Table I.

1) Bipolar PWM: The scheme of the basic switching technique for the H-bridge converter is shown in Fig. 6. Switch pairs S_{A1}, S_{B2}, S_{A2}, and S_{B1} are controlled in a complementary fashion. Therefore, two output voltage v_{conv} levels can be obtained: $-V_{DC}$ and $+V_{DC}$. The common-mode

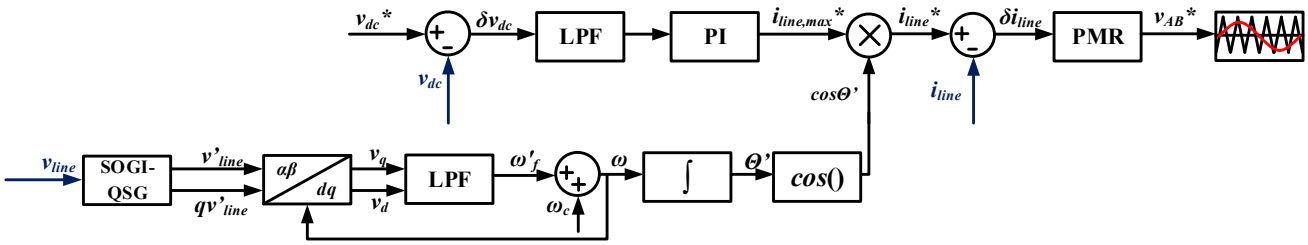

Fig. 5. Control scheme for the H-bridge converter.

voltage is nearly constant because zero-voltage state does not exist. The common-mode voltage varies only with low frequency grid voltage, but neither these changes nor dead-time influence are considered in this paper. The RMS value of leakage current i_{cm} is very low. The turn-on sequence for the positive line voltage can be presented as D_{A2}+D_{B1}, S_{A1}+S_{B2}, and D_{A2}+D_{B1}, where letter D denotes a freewheeling diode. Unfortunately, because of bipolar switching, this scheme imposes high voltage stress and high inductor current ripple, which is associated with additional losses.

2) Unipolar PWM: Setting a reference signal for every converter leg independently and with 180° phase shift results in a zero-voltage state in the middle of each switching period, which, in turn, results in unipolar transition between "active" states that correspond to three values of converter output voltage v_{conv}: -V_{DC}, 0, and +V_{DC}. Hence, switching frequency is effectively doubled. Unipolar switching also reduces dv/dt stress on the system. Both features reduce the size of the filtering components. In terms of the turn-on sequence, i.e., D_{A2}+S_{B2}, S_{A1}+S_{B2}, S_{A1}+D_{B1}, S_{A1}+S_{B2}, D_{A2}+S_{B2}, the switching losses are the same as in the bipolar modulation (P_{sw} =1 pu). Although more transitions per switching period exist, only one device changes state in each of them. Therefore, the effective number of switching becomes the same. Despite having natural advantages over bipolar modulation, this scheme is far less suitable for any transformerless PV application because every switching action is "mirrored" in the v_{CM} voltage, which changes between 0, V_{DC}/2, and V_{DC}, as shown in Fig. 7. This phenomenon causes high i_{cm} current to flow, which disqualifies unipolar PWM from this application.

3) Conventional Hybrid PWM: The idea of hybrid modulation is based on switching both legs independently and with different frequencies. The first leg is modulated with low fundamental grid frequency, whereas the second leg operates with the normal high switching frequency. Similar to the unipolar scheme, three voltage levels can be obtained. In terms of the switching pattern (Fig. 8), turn-on sequence D_{A2}+S_{B2}, S_{A1}+S_{B2}, D_{A2}+S_{B2} is similar to the unipolar modulation, except for the lack of the zero-voltage state in the middle of a switching period. The switches of leg B change their state every half-cycle of the line voltage. For this reason, switch losses are two times lower (P_{sw}=0.5 pu) than that of previous schemes. The common-mode voltage also

TABLE I
PWM TECHNIQUE COMPARISON

Modulation technique	Switching losses P_{sw} (pu)	v_{CM} variations
Bipolar	1	≈ $V_{dc}/2$ ≈ const.
Unipolar	1	0,$V_{dc}/2$, V_{dc}
Conventional Hybrid	0.5	0,$V_{dc}/2$, V_{dc}
Proposed Hybrid	0.5	0, $V_{dc}/2$

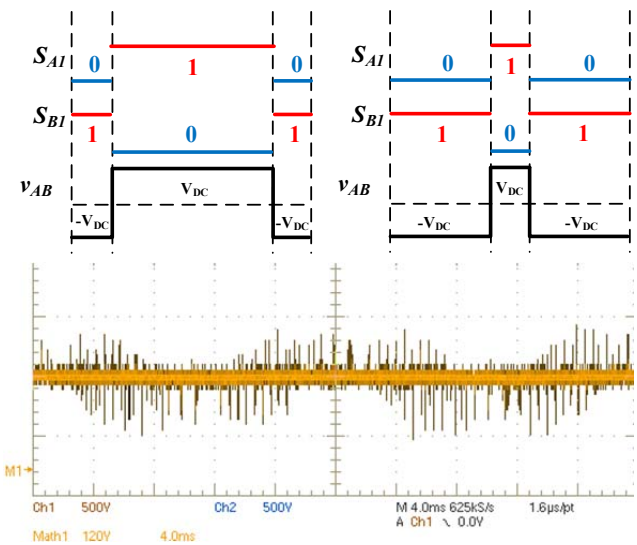

Fig. 6. Switching states and common-mode voltage v_{CM} waveform for the bipolar modulation (switching states S_{A2} and S_{B2} are negations of S_{A1} and S_{B1}, respectively).

varies between 0, V_{DC}/2, and V_{DC} but with superimposed square-shape waveform with the frequency of the v_{line} voltage (50 Hz in this case). Very fast voltage changes every half of the cycle result in high current spikes combined with large oscillations because of the LC resonant tank formed both by filtering components and parasitic capacitance of a PV array. Therefore, this technique also cannot be utilized in a transformerless system.

B. Modification of a Hybrid PWM

As discussed in the previous section, none of the modulation techniques can be suitably used in simple

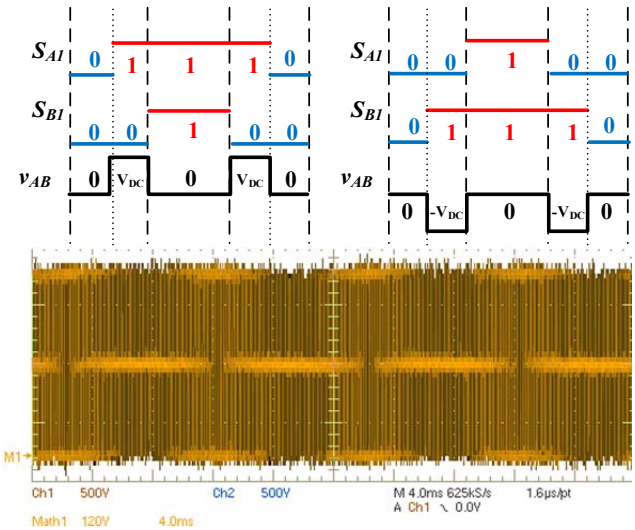

Fig. 7. Switching states and common-mode voltage v_{CM} waveform for unipolar modulation (switching states S_{A2} and S_{B2} are negations of S_{A1} and $S_{B1,}$ respectively).

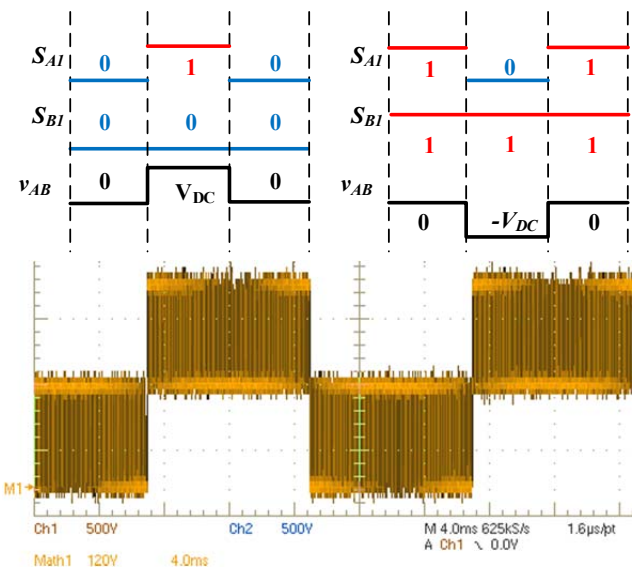

Fig. 8. Switching states and common-mode voltage v_{CM} waveform for the conventional hybrid modulation (switching states S_{A2} and S_{B2} are negations of S_{A1} and $S_{B1,}$ respectively).

transformerless PV applications. Despite constant v_{CM}, bipolar modulation results in poor efficiency because of high switching losses and grid-side filtering requirements. Unipolar modulation exhibits very strong variations in v_{CM}. Hybrid modulation seems to be most promising because of the lowest switching losses. However, the 50 Hz square waveform v_{CM} induces large oscillations both in line and leakage current. To minimize large spikes generated every half of a line voltage period, a modification has been introduced into a hybrid modulation switching pattern. Unlike in the conventional technique, only one zero-voltage state is used during the converter operation (Fig. 9). In practical

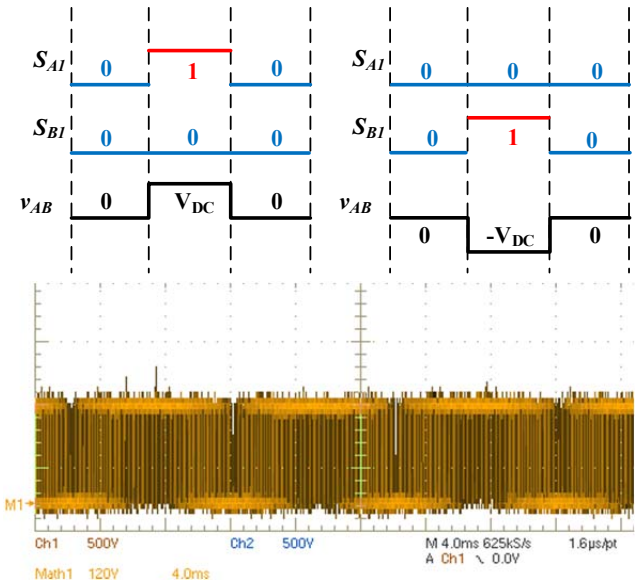

Fig. 9. Switching states and common-mode voltage v_{CM} waveform for the proposed hybrid modulation (switching states S_{A2} and S_{B2} are negations of S_{A1} and S_{B1}, respectively).

Fig. 10. System prototype: boost converter (2 strings)+ H-bridge converter: 1- TMS320F28069 board with control panel; 2- input filter; 3- boost converter inductors; 4- output filter; and 5- RFI filter.

implementation, the operation interchanges the switching patterns between fast- and slow-switching legs in the converter depending on the line voltage sign. In other words, every half-cycle of the line voltage, high-frequency switching is assigned from one converter leg to another. Thus, only transitions from 0 to $V_{DC}/2$ are present in the v_{CM} voltage waveform.

No square-shaped waveform is generated; thus, high current spikes and oscillations are avoided and stable operation is assured. The switching pattern for a positive line voltage is exactly the same, i.e., D_{A2}+S_{B2}, S_{A1}+S_{B2}, and D_{A2}+S_{B2}. Total power losses in the semiconductor devices remain unchanged. Nevertheless, the overall efficiency of the converter is increased because of the absence of unwanted oscillations.

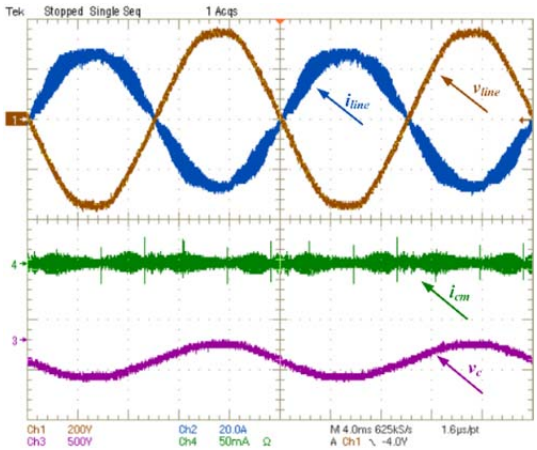

Fig. 11. Grid-connected operation with bipolar modulation: line voltage v_{line}, line current i_{line}, leakage current i_{CM}, and voltage across parasitic capacitance v_c.

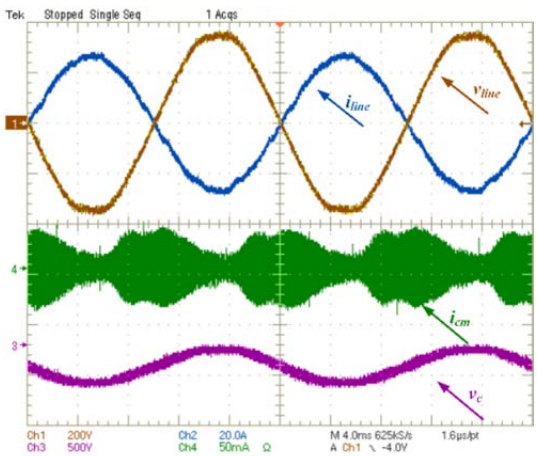

Fig. 12. Converter operation with unipolar modulation: line voltage v_{line}, line current i_{line}, leakage current i_{CM}, and voltage across parasitic capacitance v_c.

V. Experimental Study

To verify the behavior of the proposed system, experimental results were obtained with the prototype model of the converter system, as shown in Fig. 10. Instead of the PV array, the DC power supply with both voltage and current control capability was utilized. Parasitic capacitance was modeled by a branch of 15 nF/kW capacitors connected between the DC power supply negative terminal and neutral leg of the converter. The prototype contains the following: integrated DC-DC and DC-AC converters, common-mode filters, leakage current monitoring sensor, and control board based on Texas Instruments DSP TMS320F28069. The switches in both converters are Fairchild IGBTs FGH75T65UPD (650 V, 75 A). The most important parameters of the system are listed in Table II. The entire setup was developed and tested in ZE TWERD power electronics company and is now commercially available in the power range of 2–5.5 kW. Aside from leakage current

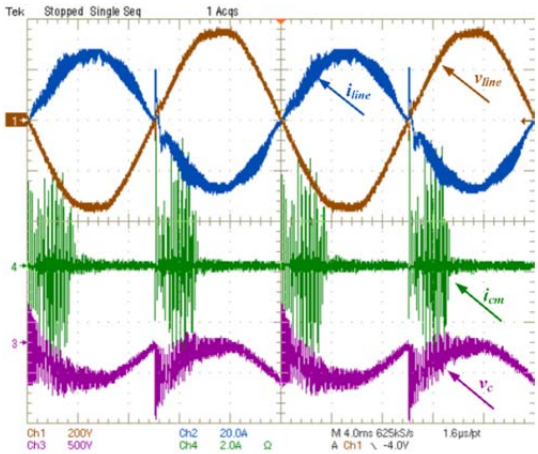

Fig. 13. Converter operation with conventional hybrid modulation: line voltage v_{line}, line current i_{line}, leakage current i_{CM}, and voltage across parasitic capacitance v_c.

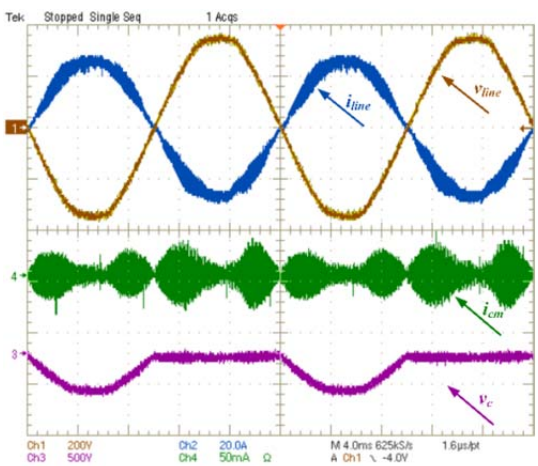

Fig. 14. Converter operation with the proposed hybrid modulation: line voltage v_{line}, line current i_{line}, leakage current i_{CM}, and voltage across parasitic capacitance v_c.

measurement, converter efficiency and THD of line current were obtained. Total converter efficiency was measured with a Yokogawa WT1806 High-Performance Power Analyzer at nominal power of 5.5 kW. Every modulation scheme described in the previous section was tested using the same filtering elements. Sampling frequency was set to 16 kHz, which, in case of unipolar modulation, implies that the effective switching frequency was 32 kHz. Figures 11-14 show grid-connected operation of the converter with leakage current i_{CM} and voltage measured on a parasitic capacitance v_c. Detailed values obtained for every modulation scheme are shown in Table III. The leakage current has the lowest value for bipolar modulation because of nearly constant common-mode voltage v_{CM} (Fig. 11).

Unipolar modulation generates v_{CM} variations, thereby resulting in the highest i_{CM} value (Fig. 12). However, because common-mode filters are employed, both PWM techniques result in i_{CM} values that are below the limit set in

TABLE II
SYSTEM PARAMETERS

Rated power	5.5 kW
Switching device	FGY75N60SMD
Sampling frequency f_s	16 kHz
DC-link capacitance C_{DC}	3 mF
Input capacitance C_{boost}	1mF / string
DC-DC inductor L_{boost}	1 mH / string
DC-AC output inductor L_{line}	2 x 0.6 mH
Common-mode filter capacitors $C_{A+/A-/B+/B-}$	2 µF
Common-mode inductors L_{cm}	2 x 300 µH
PV parasitic capacitance C_{PV}	15 nF / kW

TABLE III.
RESULTS FOR GRID-CONNECTED OPERATION AT 5.5 KW

Modulation technique	$I_{cm,RMS}$ **[mA]**	**η [%]**	**THD [%]**
Bipolar	8	96.52	4.1
Unipolar	23.1	96.68	3.5
Conventional hybrid	386*	95.79*	6.8*
Proposed Hybrid	16	97.2	3.2

$I_{cm,RMS}$: RMS value of leakage current i_{CM}, converter efficiency η, and THD of line current i_{line}.
* Value obtained with resonance occurring (Fig. 11)

VDE0126-1-1. In conventional hybrid modulation (Fig. 13), 50 Hz changes superimposed on v_{CM} result in large i_{CM} current spikes and oscillations every half cycle of the line. Therefore, its RMS value is much higher compared with the other techniques. For the same reason, efficiency and THD measurements were considered unreliable.

As shown in Fig. 14, the leakage current of the proposed modulation technique is smaller than that of the unipolar and conventional hybrid modulations. Parasitic capacitance voltage v_c for the proposed modulation techniques exhibit a half-wave shape that corresponds to only one zero-voltage state utilized for operation. The proposed hybrid PWM has two major advantages over other PWM schemes. First, it eliminates the oscillation problem. Therefore, it is applicable to the system while maintaining its most important feature: its high efficiency. Second, it allows for approximately 30% reduction of i_{CM} compared with the unipolar PWM. Finally, the THD of the line current for the proposed modulation was less than 5%, and efficiency was above 97%, which served as the main criteria for the system design.

VI. CONCLUSION

A simple technique that reduces leakage current in a highly efficient converter for PV generation has been described in this paper. Both goals of this study are achieved by employing an appropriate hybrid modulation that reduces switching losses and by adding common-mode filters at the DC and AC sides of the system, which reduces the leakage current value well below limits set by the VDE0126-1-1 standard. For conventional hybrid PWM, these filters create a resonant tank with other system components, thus practically eliminating the errors from such application. Simple modification in the hybrid PWM technique solves the aforementioned problem and results in additional decrease in leakage current. Most importantly, without modifying the converter topology and violating existing patents, low leakage current and THD of the line current are obtained, which is a significant advantage of the proposed system.

ACKNOWLEDGMENT

This work was supported in part by the Polish Federation of Engineering Associations (NOT) under Grant ROW-III-108/2010; the Institute of Control and Industrial Electronics, Warsaw University of Technology, Warsaw, Poland; and ZE TWERD Power Electronics Company.

REFERENCES

[1] T. K. S. Freddy, N. A. Rahim, W.-P. Hew, and H. S. Che, "Comparison and analysis of single-phase transformerless grid-connected PV inverters," *IEEE Trans. Power Electron.*, Vol. 29, No. 10, pp. 5358-5369, Oct. 2014

[2] D. Meneses, F. Blaabjerg, O. García, and J. A. Cobos, "Review and comparison of step-up transformerless topologies for photovoltaic AC-module application," *IEEE Trans. Power Electron*., Vol. 28, No. 6, pp. 2649-2663, Jun. 2013.

[3] R. Teodorescu, M. Liserre, and P. Rodrguez, *Grid Converters for Photovoltaic and Wind Power Systems*, Wiley-IEEE Press, 2011.

[4] O. Lopez, R. Teodorescu, F. Freijedo, and J. D. Gandoy, "Leakage current evaluation of a single phase transformerless PV inverter connected to the grid," *Applied Power Electronics Conference, APEC 2007-Twenty Second Annual IEEE*, pp. 907-912, 2007.

[5] T. Kerekes., "Analysis and modeling of transformerless photovoltaic inverter systems," PhD Thesis, Aalborg University, Aalborg, Denmark, 2009.

[6] X. Huafeng, S. Xie, Y. Chen, and R. Huang, "An optimized transformerless photovoltaic grid-connected inverter," *IEEE Trans. Ind. Electron.*, Vol. 58, No. 5, pp. 1887-1895, May 2011.

[7] G. Buticchi, D. Barater, E. Lorenzani, and G. Franceschini, "Digital control of actual grid-connected converters for ground leakage current reduction in PV transformerless systems," *IEEE Trans. Ind. Informat.*, Vol. 8, No. 3, pp. 563-572, Aug. 2012.

[8] Y. Yongheng, F. Blaabjerg, and H. Wang, "Low-voltage ride-through of single-phase transformerless photovoltaic inverters," *IEEE Trans. Ind. Appl.*, Vol. 50, No. 3, pp. 1942-1952, May/Jun. 2014.

[9] T. Friedli, M. Hartmann, and J. W. Kolar, "The essence of three-phase PFC rectifier systems — Part II," *IEEE Trans.*

Power Electron., Vol. 29, No. 2, pp. 543-560, Feb. 2014.
[10] D. Dong; L. Fang D. Boroyevich, and P. Mattavelli, "Leakage current reduction in a single-phase bidirectional AC–DC full-bridge inverter," *IEEE Trans. Power Electron.*., Vol. 27, No. 10, pp. 4281-4291, Oct. 2012.
[11] T. Esram and P. L. Chapman, "Comparison of photovoltaic array maximum power point tracking techniques," *IEEE Trans. Energy Convers*., Vol. 22, No. 2, pp. 439-449, Jun. 2007.
[12] M. A. G de Brito, L. Galotto, L. P. Sampaio, G. de Azevedo e Melo, and C. A. Canesin, "Evaluation of the main MPPT techniques for photovoltaic applications," *IEEE Trans. Ind. Electron*., Vol. 60, No. 3, pp. 1156-1167, Mar. 2013.
[13] D. Sera, L. Mathe, and T. Kerekes, S.V Spataru, and R. Teodorescu, "On the perturb-and-observe and incremental conductance MPPT methods for PV systems," *IEEE J. Photovolt.*, Vol. 3, No. 3, pp. 1070-1078, Jul. 2013.
[14] A. K. Abdelsalam, A. M. Massoud, S. Ahmed, and P. Enjeti, "High-performance adaptive perturb and observe MPPT technique for photovoltaic-based microgrids," *IEEE Trans. Power Electron*., Vol. 26, No. 4, pp. 1010-1021, April 2011
[15] F. Scarpetta, M. Liserre, and R.A Mastromauro, "Adaptive distributed MPPT algorithm for photovoltaic systems," *IECON 2012 - 38th Annual Conference on IEEE Industrial Electronics Society*, pp. 5708-5713, 2012.
[16] L. Hadjidemetriou, E. Kyriakides, and F. Blaabjerg, "A new hybrid PLL for interconnecting renewable energy systems to the grid," *IEEE Trans. Ind. Appl.*, Vol. 49, No. 6, pp. 2709-2719, Nov./Dec. 2013.
[17] F. Blaabjerg, R. Teodorescu, M. Liserre, and A.V. Timbus, "Overview of control and grid synchronization for distributed power generation systems," *IEEE Trans. Ind. Electron*., Vol. 53, No. 5, pp. 1398-1409, Oct. 2006
[18] S. Stynski, "Analisys and control of muitilevel AC-DC-AC flying capacitor converter fed trom single-phase grid," PhD Thesis, Warsaw University of Technology, Warsaw, Poland, 2012.
[19] R. Teodorescu, F. Blaabjerg, M. Liserre, and P.C Loh, "Proportional-resonant controllers and filters for grid-connected voltage-source converters," *IEE Proc. Electric Power Applications*, Vol. 153, No. 5, pp. 750-762, 2006.

Radoslaw Kot received his M.Sc. degree in electrical engineering from the Department of Electrical Engineering, Warsaw University of Technology (WUT), Warsaw, Poland, in 2010. He is currently working toward his Ph.D. degree at the Institute of Control and Industrial Electronics (WUT). His research interests include renewable energy conversion systems, power converters topologies, and control design. He has been involved in several research and industrial projects. He is a member of the IEEE Industrial Electronics Society.

Sebastian Stynski received his M.Sc. and Ph.D. degrees in electrical engineering (with awards) from Warsaw University of Technology (WUT), Warsaw, Poland, in 2006 and 2012, respectively. While working toward his Ph.D. degree, he became a Scholar of the Center for Advanced Studies for Ph.D. students and young doctors (2008–2010) under the project "Development Programme of Warsaw University of Technology" and a recipient of scholarship from the Foundation for Polish Science Ventures Programme (2009–2011). In 2010, he received Team Award of the Rector of the Warsaw University of Technology for his scientific achievements. He received an award from TRUMPF Huettinger Company and Faculty of Electronics and Information Technology, WUT, for publishing the best Ph.D. thesis in 2012. Since 2013, he has been with the Institute of Control and Industrial Electronics, WUT. In 2014, he received a prestigious Scholarship (2014–2017) from the Polish Ministry of Science and Higher Education. His research interests include modulation techniques and control methods of single and multiphase multilevel converters, resistance of power electronics systems on different grid disturbances, and power electronics interfaces between renewable energy sources and grid. His scientific achievements include participating in more than 20 research and industrial projects; he served as project leader in five of these projects. He is an author and co-author of more than 40 technical papers and reports, including 4 chapters in books and journal papers indexed by TR JCR. He is an active member of the IEEE within the Poland IEEE Industrial Electronics and Power Electronics Joint Chapter PEL-035/IEL-013, where he is the current Chairman.

Krzysztof Stepien received his M.Sc. degree in technical physics from the Faculty of Physics, Astronomy and Informatics, Nicolaus Copernicus University, Torun, Poland. He is currently a manager of Frequency Converters for Renewable Energy Sources Department in ZE TWERD Company, Torun, Poland.

Jaroslaw Zaleski received his M.Sc. degree in electrical engineering from the Faculty of Electrical and Control Engineering, Gdansk University of Technology, Gdansk, Poland, in 1994. He is currently a technical director in ZE TWERD power electronics company, Torun, Poland. His contribution to series of industry converters resulted in awards and medals during the Innovation Exhibition in Geneva in 2006 and the Exhibition in Brussels "Eureco" in 2006.

Mariusz Malinowski received his Ph.D. and D.S. degrees in electrical engineering from the Institute of Control and Industrial Electronics, Warsaw University of Technology (WUT), Warsaw, Poland, in 2001 and 2012, respectively. He was a visiting scholar at Aalborg University, Aalborg, Denmark; the University of Nevada, Reno, NV, USA; the Technical University of Berlin, Berlin, Germany; and ETH Zurich, Zurich, Switzerland. He was a visiting professor at Universidad Tecnica Federico Santa Maria, Valparaíso, Chile; the University of CergyPontoise, Cergy-Pontoise, France; and École Nationale Supérieure d'Électronique, d'Électrotechnique, d'Informatique, d'Hydraulique, et des Télécommunications–Laplace, Toulouse, France. He is currently with the Institute of Control and Industrial Electronics, WUT. His current research interests include control and modulation of grid-side converters, multilevel converters, smart grids, and power generation systems

based on renewable energies. He has co-authored more than 130 technical papers and 6 books. He holds two implemented patents. Prof. Malinowski was the recipient of the Siemens Prize in 2002 and 2007; the WUT President Prize in 2001, 2005, 2007, 2009, 2011, and 2013; the Paper Award at the Industrial Electronics Conference 2000 and the European Power Electronics—Power Electronics and Motion Control 2004; the Polish Minister of Science and the Higher Education Awards in 2003 and 2008; the Prime Minister of Poland Award for Habilitation in 2013; and the IEEE Industrial Electronics Society (IES) David Irwin Early Career Award for Outstanding Research and Development of Modulation and Control for Industrial Electronics Converters in 2011. He received several awards and medals during the Innovation Exhibition in Geneva in 2006 and the Exhibition in Brussels "Eureco" in 2006. He is currently the IES Vice President (VP) for Workshops Activities and the VP of the Poland Section of IEEE. He is an associate editor of IEEE Transactions on Industrial Electronics, IEEE Transactions on Power Electronics, and was the editor-in-chief of the IEEE Industrial Electronics Magazine from 2010 to 2012.